

Implications of multiwavelength spectrum on cosmic-ray acceleration in blazar TXS 0506+056

Saikat Das¹, Nayantara Gupta², and Soebur Razzaque^{3,4,5}

¹ Center for Gravitational Physics, Yukawa Institute for Theoretical Physics, Kyoto University, Kyoto 606-8502, Japan
e-mail: saikat.das@yukawa.kyoto-u.ac.jp

² Astronomy & Astrophysics Group, Raman Research Institute, Bangalore 560080, Karnataka, India
e-mail: nayan@rri.res.in

³ Centre for Astro-Particle Physics (CAPP) and Department of Physics, University of Johannesburg, PO Box 524, Auckland Park 2006, South Africa
e-mail: srazzaque@uj.ac.za

⁴ Department of Physics, The George Washington University, Washington, DC 20052, USA

⁵ National Institute for Theoretical and Computational Sciences (NITheCS), South Africa

Received YYYY; accepted ZZZZ

ABSTRACT

Context. The MAGIC collaboration has recently analyzed data from a long-term multiwavelength campaign of the γ -ray blazar TXS 0506+056. In December 2018, it was flaring in the very-high-energy (VHE; $E > 100$ GeV) γ -ray band, but no simultaneous neutrino event was detected.

Aims. We model the observed spectral energy distribution (SED), using a one-zone leptohadronic emission.

Methods. We estimate the neutrino flux through the restriction from observed X-ray flux on the secondary radiation due to hadronic cascade, initiated by protons with energy $E_p \lesssim 0.1$ EeV. We assume ultrahigh-energy cosmic rays (UHECRs; $E \gtrsim 0.1$ EeV), with the same slope and normalization as the low-energy spectrum, are accelerated in the jet but escape efficiently. We propagate the UHE protons in a random, turbulent extragalactic magnetic field (EGMF).

Results. The leptonic emission from the jet dominates the GeV range, whereas the cascade emission from CR interactions in the jet contributes substantially to the X-ray and VHE range. The line-of-sight cosmogenic γ rays from UHECRs produce a hardening in the VHE spectrum. Our model prediction for neutrinos from the jet is consistent with the 7.5-year flux limit by IceCube and shows no variability during the MAGIC campaign. Therefore, we infer that the correlation between GeV-TeV γ -rays and neutrino flare is minimal. The luminosity in CRs limits the cosmogenic γ -ray flux, which, in turn, bounds the RMS value of the EGMF to $\gtrsim 10^{-5}$ nG. The cosmogenic neutrino flux is lower than the IceCube-Gen2 detection potential for 10 yrs of observation.

Conclusions. VHE γ -ray variability should arise from increased activity inside the jet; thus, detecting steady flux at multi-TeV energies may indicate UHECR acceleration. Upcoming γ -ray imaging telescopes, such as the CTA, will be able to constrain the cosmogenic γ -ray component in the SED of TXS 0506+056.

Key words. Astroparticle physics – galaxies: active – gamma-rays: general – neutrinos

1. Introduction

Blazars are a subclass of radio-loud Active Galactic Nuclei (AGNs), with their highly relativistic jet collimated towards the observer's line of sight. They have been considered as prominent candidates for the origin of IceCube-detected diffuse astrophysical neutrino flux beyond ~ 10 TeV (IceCube Collaboration et al. 2013; Eichler 1979; Sikora et al. 1987; Petropoulou et al. 2015; Murase et al. 2018; Yuan et al. 2020) and may also contribute in the PeV-EeV energy range (Kalashev et al. 2013; Kochowski et al. 2021; Das et al. 2021). For the first time in September 2017, a high-energy muon-neutrino event IC-170922A ($E_\nu \sim 0.3$ PeV) was associated with the γ -ray flaring blazar TXS 0506+056 at 3σ significance (Aartsen et al. 2018a). Subsequently, other events having positional coincidence with Fermi-LAT detected blazars are also observed with lower statistical significance (Garrappa et al. 2019; Franckowiak et al. 2020). Despite several studies on this object, it is crucial to revisit the spectral properties for predicting the multi-messenger signals from similar sources.

The explanation of the neutrino event requires synchrotron (SYN) and synchrotron self-Compton (SSC) photons as the target for $p\gamma$ interactions (Gao et al. 2019; Cerruti et al. 2019; Sahu et al. 2020). Whereas, other models require an external photon field, resulting in external inverse-Compton (IC) emission (Reimer et al. 2019; Keivani et al. 2018; Rodrigues et al. 2019; Petropoulou et al. 2020). In the hadronuclear interpretation via pp interaction, the shock accelerated protons may interact with gas clouds in the vicinity of the supermassive black hole (Liu et al. 2019) or cold protons in the jet (Banik & Bhadra 2019). Some studies invoke neutrino production from the interaction of relativistic neutron beams in the jet, originating in $p\gamma$ interactions with external photons (see for e.g., Zhang et al. 2020). In Fraija et al. (2020), $p\gamma$ interactions occur with seed photons produced by annihilation of electron-positron pairs from the accretion disk.

The CR-induced cascade from Bethe-Heitler (BH) pair production contributes near the X-ray energies in the $p\gamma$ scenario, thus also limiting the hadronic component in GeV-TeV γ -rays. As a result, this constrains the astrophysical neutrinos,

in many cases, to a flux level lower than predicted by IceCube observations. Thus, an additional photon field of energy $\epsilon \simeq m_\pi m_p c^4 / 20E_\nu \simeq 440$ eV, i.e., in the UV to soft X-ray energy band, is required. However, an “orphan” neutrino flare from this source from September 2014 to March 2015 is revealed from the analysis of archival data, at 3.5σ statistical significance (Aartsen et al. 2018b) with 13 ± 5 signal events above the atmospheric background. The latter was not accompanied by increased activity in γ -rays, indicating different astrophysical processes may dominate for neutrino and γ -ray flares. Often, a two-zone model is employed, considering a high opacity for GeV γ -rays in the neutrino production region (Sahakyan 2018; Xue et al. 2019, 2021).

Recently, the MAGIC collaboration has modeled the spectrum of TXS 0506+056, observed during a multiwavelength campaign lasting 16 months from November 2017 to February 2019, covering the radio band, optical/UV, high-energy, and very-high-energy (VHE, $E > 100$ GeV) γ -rays (Acciari et al. 2022). A γ -ray flaring activity was observed by MAGIC during December 2018. Fermi-LAT observed several short flares on timescales of days to weeks, unlike the long-term flare of 2017. At lower energies, no significant variability was observed. The observed flare was not associated with any neutrino event. Their model infers the neutrino luminosity to be lower than the detection threshold of currently operating instruments.

We analyze the multiwavelength SED using a one-zone leptohadronic model. The low-energy peak results from the SYN radiation of relativistic electrons. The high-energy peak is produced by SSC and IC scattering of external photons (external Compton, abbrev. EC). These external photons may originate from the broad-line region (BLR). Although a broad-line emission in the optical spectrum is not detected, TXS 0506+056 can be a masquerading BL Lac, i.e., intrinsically a flat spectrum radio quasar (FSRQ) with hidden broad lines and a standard accretion disk (Padovani et al. 2019). The interaction of the cosmic ray protons with the leptonic radiation and the external photon field produces a characteristic photon spectrum resulting from the electromagnetic cascade of secondary electrons, which is constrained by the X-ray data.

Blazars are also suitable candidates for ultrahigh-energy cosmic ray (UHECR; $E \gtrsim 10^{18}$ eV) acceleration. They can escape the jet and interact with cosmic background photons. In an earlier work, the neutrino flux originating in extragalactic propagation of UHECRs from TXS 0506+056, and a few other blazars was analyzed (Das et al. 2022). We assumed a correlation between the cosmic-ray and IceCube-detected neutrino luminosity inside the jet, to scale the cosmogenic fluxes. Here, we constrain the UHECR luminosity by SED modeling, consistently with the allowed flux of cosmogenic γ -rays. The EGMF is crucial to determine this line-of-sight resolved γ -ray component. Using the latest spectrum data, we coherently explain the multiwavelength SED, and predict the corresponding neutrino flux from the jet emission region, and the plausibility of cosmogenic γ -ray contribution to the SED. Finally, the luminosity constraint can be used to predict the resulting cosmogenic neutrino flux at EeV energies.

The observed multiwavelength SED is difficult to resolve into components coming from interactions inside the jet or line-of-sight resolved UHECR interactions, or multiple zones, etc. Hence all photons are treated on equal footing by the detectors. Thus, if UHECRs escape from the source, they produce cosmogenic gamma-rays and the line-of-sight resolved component of that flux can contribute at the VHE range of the MWL SED. We invoke three components (i) a purely leptonic emission (ii)

hadronic emission inside the jet (iii) a line-of-sight component of the hadronic emission during extragalactic propagation. This is the reason the cosmogenic gamma-ray spectrum is also used to fit the observed SED.

Our study is essentially a one-zone model, with all the jet parameters constrained by the MWL SED. These jet parameters are used to calculate the luminosity in cosmic rays required inside the jet for SED and neutrino modeling. However, the parameter space is degenerate and hence adjusted to maximize the neutrino production inside the jet. Now, using the same normalization of the proton spectrum required for this luminosity, we also calculate the luminosity in escaping UHECRs. Hence, it is essentially the same proton spectrum, with the same normalization. But, we assume at energies $\gtrsim 0.1$ EeV they escape the source, because the observed SED does not allow for UHECR interactions inside the source and simultaneous explanation of quiescent state neutrino flux.

We present the methods of our one-zone modeling in Sec. 2. In Subsec. 3.1 we present the results for leptohadronic emissions inside the jet. In Subsec. 3.2 we show the contribution of line-of-sight resolved cosmogenic γ -ray contribution to the SED and the subsequent constraints on the EGMF strength. We discuss our results and draw our conclusions in Sec. 4.

2. Radiative Modeling

We consider the emission region in the jet to be a spherical blob of radius R' , consisting of a relativistic plasma of electrons and protons moving through a uniform magnetic field B . The bulk Lorentz factor of the jet is Γ and the doppler factor is given by $\delta_D = [\Gamma(1 - \beta \cos \theta)]^{-1}$, where βc is the velocity of the emitting plasma and θ is the viewing angle. For $\theta \lesssim 1/\Gamma$, $\Gamma \approx \delta_D$. We inject electrons in the blob with a spectrum

$$Q'_e(\gamma'_e) = A_e(\gamma'_e/\gamma_0)^{-\alpha-\beta \log_{10}(\gamma'_e/\gamma_0)} \quad \text{for } \gamma'_{e,\min} < \gamma'_e < \gamma'_{e,\max} \quad (1)$$

to fit the observed broadband SED. The normalization of the spectrum A_e depends on the luminosity of injected electrons, and $\gamma_0 m_e c^2$ is a reference energy fixed at 500 MeV. A quasi-steady state is reached when the injection is balanced by radiative cooling and/or escape. Empirically, the steady state electron density distribution is given as $N'_e(\gamma'_e) = Q'_e(\gamma'_e)t'_e$, where $t'_e = \min\{t'_{\text{cool}}, t'_{\text{esc}}\}$. We consider the escape timescale $t'_{\text{esc}} \simeq t'_{\text{dyn}} = 2R'/c$. The radiative cooling timescale is given as

$$t'_{\text{cool}} = \frac{3m_e c}{4(u'_B + \kappa_{\text{KN}} u'_{\text{ph}}) \sigma_T \gamma'_e} \quad (2)$$

Here $u'_B = B^2/8\pi$ is the energy density in magnetic field, u'_{ph} is the energy density of soft photons, σ_T is the Thomson scattering cross-section, and κ_{KN} accounts for the suppression of IC emission due to the Klein-Nishina effect. We use the open-source code GAMERA to solve the transport equation for obtaining the injection spectrum at time t' (Hahn 2016),

$$\frac{\partial N'_e}{\partial t} = Q'_e(\gamma'_e, t') - \frac{\partial}{\partial \gamma'_e}(b N'_e) - \frac{N'_e}{t'_{\text{esc}}} \quad (3)$$

where $b = b(\gamma'_e, t')$ is the energy loss rate of electrons.

The steady-state electron spectrum yields the SYN and SSC emission. In addition, we consider an external photon field, which is Compton upscattered by the same electrons. It is considered to be a blackbody with temperature T' and energy density $u'_{\text{ext}} = (4/3)\Gamma^2 u_{\text{ext}}$ in the jet frame, where the energy density

in the AGN frame is $u_{\text{ext}} = \eta_{\text{ext}} L_{\text{disk}} / 4\pi R_{\text{ext}}^2 c$ and η_{ext} is the fraction of the disk luminosity. Here R_{ext} is the radius of the region containing the external photons. The emission blob is assumed to be at this distance along the axis of the jet. These photons can enter the relativistic jet and become doppler boosted in the comoving frame.

The steady state proton injection spectrum is given by a power-law $N'_p(\gamma'_p) = A_p \gamma'^{-\alpha}_p$. The main energy loss processes of the protons are pion production ($p\gamma \rightarrow p + \pi^0$ or $n + \pi^+$) and BH process ($p\gamma \rightarrow p + e^+e^-$). The seed photons are the leptonic emission and external photons. The charged pions decay to produce neutrinos. The timescale of these interactions can be expressed as follows

$$\frac{1}{t'_{p\gamma}} = \frac{c}{2\gamma'^2_p} \int_{\epsilon_{\text{th}}/2\gamma_p}^{\infty} d\epsilon'_\gamma \frac{n(\epsilon'_\gamma)}{\epsilon'^2_\gamma} \int_{\epsilon_{\text{th}}}^{2\epsilon\gamma_p} d\epsilon_r \sigma(\epsilon_r) K(\epsilon_r) \epsilon_r \quad (4)$$

where $\sigma(\epsilon_r)$ and $K(\epsilon_r)$ are the cross-section and inelasticity respectively of photopion production or BH pair production as a function of photon energy ϵ_r in the proton rest frame. $n(\epsilon'_\gamma)$ is the target photon number density (Stecker 1968; Chodorowski et al. 1992; Mücke et al. 2000). The interaction timescale of protons inside the jet is many orders of magnitude higher than the dynamical timescale, below tens of PeV energies. Hence, in order to increase the efficiency of $p\gamma$ interactions required for appreciable neutrino production, it is compelling to ignore their escape if the Eddington luminosity budget is maintained. Otherwise, the production of same neutrino flux will require higher kinetic power in protons, if the escape rate is comparable to $p\gamma$ interaction rate. Hence, an escape timescale higher than the $p\gamma$ interaction timescale is assumed. The normalization A_p of the proton spectrum is calculated from the luminosity requirement arising from the in-jet hadronic contribution to the SED.

The spectrum of γ rays from the decay of neutral pions and the spectrum of e^+e^- due to BH process are calculated using the parametrization by Kelner & Aharonian (2008). When calculating the pion decay gamma-rays and electron spectra, the input proton spectrum is weighted by the rate of the corresponding process, for eg., in case of electron spectrum from Bethe-Heitler process, we inject $N'_p(\gamma'_p) * R_{\text{BH}}/R_{\text{tot}}$, where R_{BH} is the Bethe-Heitler interaction rate (calculated using Eqn. 4). R_{tot} is the total interaction rate considering photopion production and Bethe-Heitler pair production. The high-energy γ rays are absorbed by $\gamma\gamma \rightarrow e^\pm$ pair production with the leptonic radiation and also with the external blackbody radiation, leading to the attenuation of TeV γ -rays. The escaping γ -ray flux is given as

$$Q'_{\gamma, \text{esc}}(\epsilon'_\gamma) = Q'_{\gamma, \pi}(\epsilon'_\gamma) \left(\frac{1 - \exp(-\tau_{\gamma\gamma})}{\tau_{\gamma\gamma}} \right) \quad (5)$$

We calculate $\tau_{\gamma\gamma}$ using the formalism given by Gould & Schröder (1967) to calculate the absorption probability per unit path length for an isotropic photon field,

$$I_{\gamma\gamma}^{-1}(\epsilon'_\gamma) = \frac{1}{2} \int \int n(\epsilon'_k) \sigma_{\gamma\gamma}(\epsilon'_\gamma, \epsilon'_k, \theta) (1 - \cos \theta) \sin \theta d\theta d\epsilon'_k \quad (6)$$

where $\sigma_{\gamma\gamma}$ is the full pair-production cross-section and the $n(\epsilon'_k)$ is the combined density of soft photons and external radiation.

The high-energy electrons and positrons produced in $\gamma\gamma$ pair production ($Q'_{e, \gamma\gamma}$), charged pion decay ($Q'_{e, \pi}$), and BH process ($Q'_{e, \text{BH}}$) can initiate cascade radiation from the jet. We solve the steady state spectrum of secondary electrons $N'_{e, s}(\gamma_e)$ in the jet frame using the analytical approach of Boettcher et al. (2013), including $Q'_{e, \text{BH}}$ in the source term and the escape term to be the

same as primary electrons. In a synchrotron-dominated cascade, emission from secondary electrons is given by

$$Q'_s(\epsilon'_s) = A_0 \epsilon'^{-3/2}_s \int_1^{\infty} d\gamma'_e N'_{e, s}(\gamma'_e) \gamma'^{-2/3}_e e^{-\epsilon'_s/b\gamma'^2_e} \quad (7)$$

with $A_0 = c\sigma_T B'^2/[6\pi m_e c^2 \Gamma(4/3)b^{4/3}]$ being a normalization constant, where $b = B'/B_{\text{crit}}$ and $B_{\text{crit}} = 4.4 \times 10^{13}$ G.

Our results in Subsec. 3.1 suggests that the proton spectrum inside the source is required to be cut off beyond a specific energy to explain the multiwavelength SED. The resulting neutrino flux is thus limited by this value of $E'_{p, \text{max}}$. We model the protons to escape beyond this energy if accelerated inside their source. An energy-independent escape timescale of the order of $\sim R/c$ is sufficient for escape to dominate over photohadronic interactions inside the jet. However, considering a diffusion faster than $\propto E^1$ leads to negligible interaction efficiency beyond tens of PeV energies, in the comoving jet frame. This is reasonable when a quasi-ballistic propagation is assumed instead of diffusive propagation inside the jet emission region.

The resulting muon neutrino flux from $p\gamma$ interactions is calculated as

$$E_\nu^2 J_\nu = \frac{1}{3} \frac{V' \delta_D^2 \Gamma^2}{4\pi d_L^2} E_\nu'^2 Q'_{\nu, p\gamma} \quad (8)$$

where the factor 1/3 corresponds to neutrino oscillation and $Q'_{\nu, p\gamma}$ is the total electron and muon neutrino flux from charged pion decay in the comoving frame.

3. Results

3.1. Leptohadronic emission inside the jet

During the multiwavelength campaign, the source was monitored using the Swift-XRT, Swift-UVOT, and NuSTAR, maximizing the simultaneity of observation with the MAGIC telescope (Acciari et al. 2022). From November 2017 to February 2019, a total of ~ 79 hrs of good-quality data was collected by MAGIC. During most of this period (~ 74 hrs), the source was found to be in a low-state with average photon flux $F(> 90 \text{ GeV}) = (2.7 \pm 2.1) \times 10^{-11} \text{ erg cm}^{-2} \text{ s}^{-1}$. Fermi-LAT data was also used in the spectral analysis. For the flaring state of December 2018, only simultaneous data is obtained by Fermi-LAT and MAGIC in the GeV and VHE γ -rays, and by ASAS-SN in the optical. The integral photon flux observed by MAGIC rose by an order of magnitude compared to the low state. The most significant variability was observed in the GeV band, while the X-ray variability was found to be at a lower level. The radio, optical and UV bands showed moderate variability (Acciari et al. 2022).

The γ -ray variability timescale of TXS 0506+056 observed in October 2017 was shown to be $t_{\text{var}} \leq 10^5 \text{ s}$ (Keivani et al. 2018). The γ -ray flare of December 2018 was found to be very similar. The size of the emission region inferred from the variability is $R' \lesssim \delta_D c t_{\text{var}} / (1+z) \simeq 6.75 \times 10^{16} (\delta_D/30) (t_{\text{var}}/10^5 \text{ s}) \text{ cm}$. We assume the radius of the emission region to be 10^{16} cm and $\Gamma \approx \delta_D$ during both the high- and low-states. The value of the magnetic field was fine-tuned by fitting the optical and gamma-ray data. It is also assumed to be the same in the two states, $B' = 0.28 \text{ G}$. The muons and pions produced in hadronic interactions do not suffer significant energy losses before decaying, for this value of B' .

The luminosity distance of TXS 0506+056 is $d_L \approx 1837 \text{ Mpc}$, with a redshift of $z = 0.3365$. The total kinetic power of the jet in the AGN frame is calculated as $L_{\text{kin}} = L_e + L_p + L_B =$

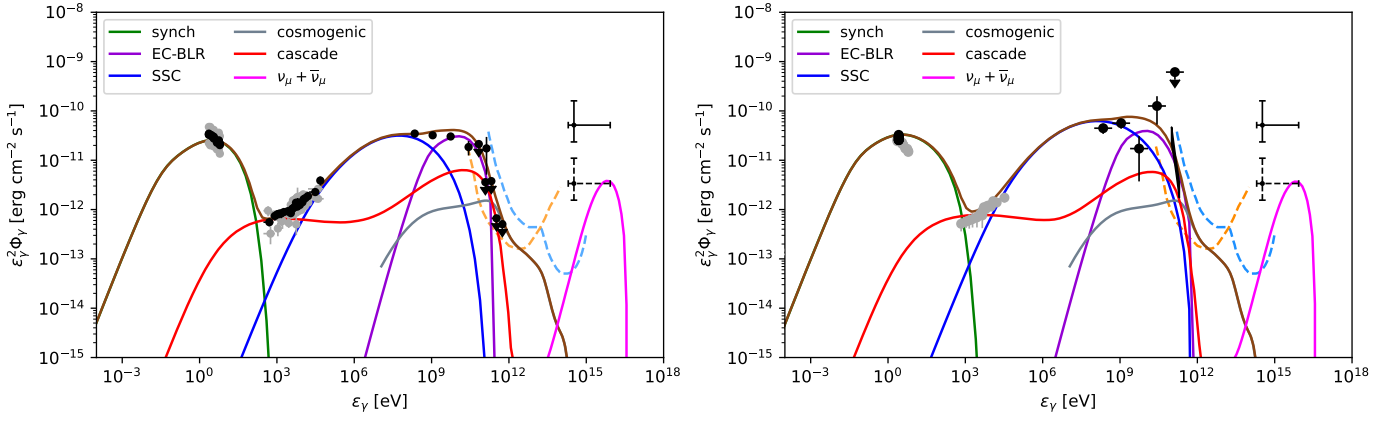


Fig. 1. Multiwavelength SED of TXS 0506+056 during the 2017-2019 campaign. *Left:* Low-state (average) flux during the observation period. Black data points show the Fermi-LAT average spectrum and MAGIC upper limits, and Swift and NuSTAR spectra on 2018 October 16. Gray data points show the whole range of optical-to-X-ray spectra. *Right:* High-state observation in VHE γ -rays during 2018 December. Black data points show the Fermi-LAT, MAGIC, and ASAS-SN contemporaneous spectra. Gray data points show the nearest observations in radio, optical, UV, and X-rays on 2018 December 8. The green, blue, and purple curves corresponds to SYN, SSC, and EC-BLR emission. The red curve is the cascade emission from secondary electrons. The magenta curve is the predicted neutrino flux in both cases. The black solid and dashed PeV data points represent the IceCube flux upper limit for one detection in 0.5 yrs and 7.5 yrs respectively for the 2017 detection event. The grey line is the cosmogenic γ -ray flux from extragalactic propagation of UHE protons. The orange and blue dashed lines are CTA and LHAASO point source sensitivity. See text for details.

Table 1. Model parameters for the multiwavelength SED, indicating the electron and proton luminosities in the AGN rest frame

Parameters	Low State	High State
δ_D	28	''
B' [G]	0.28	''
R' [cm]	10^{16}	''
u'_{ext} [erg/cm ³]	0.01	''
T' [K]	2×10^5	''
α (e/p spectral index)	2.0	''
β (log parabola index)	0.3	''
E_0 [MeV]	500	''
$E'_{e,\text{min}}$ [GeV]	0.20	0.25
$E'_{e,\text{max}}$ [GeV]	10	25
L_e [erg/s]	5.8×10^{44}	7.6×10^{44}
$E'_{p,\text{min}}$ [GeV]	10	''
$E'_{p,\text{max}}$ [PeV]	6.3	''
L_p [erg/s]	1.6×10^{48}	''

$\pi R'^2 \Gamma^2 c(u'_e + u'_p + u'_B)$, where u'_e , u'_p , and u'_B are the energy densities of electrons, protons, and magnetic field respectively. The maximum electron energy changes from $\gamma'_{e,\text{max}} = 2 \times 10^4$ in the low-state to $\gamma'_{e,\text{max}} = 5 \times 10^4$ in the high-state to account for the spectral variability. We vary the maximum proton energy ($E'_{p,\text{max}}$) in the comoving jet frame over a wide range to find the best-fit value of 6.3 PeV, fixed for both the low- and high-states. The cascade emission from the steady-state secondary electron spectrum $N'_{e,s}$ is shown by the red lines in Fig. 1. The low energy peak of the cascade emission originates from the secondary emission of e^\pm pair produced in BH process, which is severely constrained by the X-ray data. As a result the pion decay cascade at higher energies is also limited and the contribution to the high-energy peak is not significant.

We obtain $T' = 2 \times 10^5$ K and $u'_{\text{ext}} = 0.01$ erg/cm³ for the external photon field from fitting the SED, which is the most important target of py interaction for neutrino production and for IC scattering, crucial to explain the VHE spectrum. It is also vital for $\gamma\gamma$ absorption in the jet, beyond a few hundreds of GeV.

For a typical disk luminosity $L_{\text{disk}} \approx 10^{46}$ erg/s and the scattered disk emission to be a fraction $\eta_{\text{ext}} \sim 0.01$ of the disk photon energy density, R_{ext} comes out to be a few times 10^{18} cm.

The VHE flare of December 2018 does not have simultaneous observation at lower energies. Thus the constraints on the theoretical model are moderate. Nevertheless, to reduce the uncertainties, only the electron primary distribution and its corresponding luminosity is changed with respect to the low state. The parameter values used in the modeling are given in Tab. 1.

We fit the low-state spectrum first and optimize the parameters δ_D , B' , and spectral indices, using the leptonic emission only. The SYN spectrum peaks at the optical band and a log-parabola injection spectrum of electrons well explain the data. The hadronic component is then added and the power and maximum proton energy is varied to fit the X-ray data with BH cascade. The VHE photon flux upper limits constrain the contribution from the pion-decay cascade. We also consider the absorption of VHE γ -rays in the extragalactic background light (EBL) using the Gilmore et al. model (Gilmore et al. 2012). It can be seen from the left panel of Fig. 1, that the neutrino flux is comparable to the 7.5-year averaged flux prediction from this source by IceCube. We find the neutrino flux to be roughly unchanged in modeling the low- and high-state SEDs obtained by the MAGIC multiwavelength campaign. This corresponds to a flux that produces on average one neutrino detection like IC-170922A over a period of 7.5 years and explains the non-observation of neutrino events during the December 2018 flare in the MAGIC waveband. A further increase in the neutrino flux leads to the violation of the X-ray data.

3.2. Cosmogenic γ -rays from UHECRs

The maximum proton energy for photohadronic interactions in the AGN frame is $E_{p,\text{max}} = \Gamma E'_{p,\text{max}} \approx 0.17$ EeV from modeling MWL SEDs of TXS 0506+056. The proton spectrum has to be cut off at $\mathcal{O} \sim 0.1$ EeV inside the jet to satisfy constraints from X-ray data, and to simultaneously produce neutrinos with a flux in the PeV range inferred from detection of one event in 7.5 yr of IceCube operation. According to the Hillas condition,

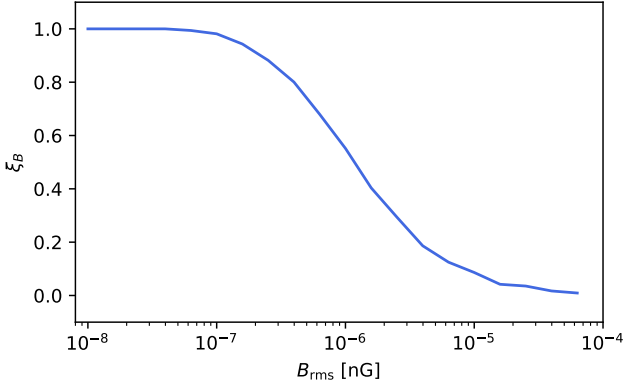


Fig. 2. Survival fraction of UHECRs along the line-of-sight, i.e., within 0.1° of the initial direction of propagation, as a function of the rms strength of EGMF.

the maximum acceleration energy $E_{p,\max}^{\text{acc}} \sim 2\beta cZeB\Gamma$, where the bulk Lorentz factor Γ takes into account the frame transformation from comoving jet frame to AGN frame. The gyration radius of 10^{20} eV protons from this simplistic expression may be calculated as $r_L \approx 2.13 \times 10^{16}$ cm, which is comparable to the blob radius in our modeling. Thus protons of energy higher than 0.17 EeV is possible to be produced in the same blob for the magnetic field and the length scale considered. The $p\gamma$ opacity in jet is higher than $1e-3$ for protons with energy $> 6 \times 10^{17}$ eV (see eg. Das et al. 2022). The jet is opaque to photons beyond ~ 1 TeV, therefore if UHE protons interact inside the jet, additional gamma-rays from π^0, π^\pm cascade would contribute at lower energies, violating the X-ray data. Hence, we assume that UHE protons beyond this energy escape the jet. A faster escape at higher rigidities has been parametrized in earlier studies. For eg., see Eqn. 20 in Harari et al. (2014) and applied to the case of inside the source in Muzio et al. (2022). Thus, it is inherently the same population of protons, which interacts below ~ 0.1 EeV and escapes at higher energy. This assumption allows us to use the same normalization of the proton spectrum inside and outside the jet, with the same injection spectral index.

Assuming that protons escape efficiently beyond ~ 0.1 EeV and up to 10^{20} eV as UHECRs, we calculate the cosmogenic γ -ray spectrum resulting from their propagation in the EGMF and interactions with the CMB and EBL photons. Secondaries from these interactions initiate electromagnetic cascade in the extragalactic medium, undergoing synchrotron radiation in the EGMF, pair production with EBL, inverse IC scattering of background photons, etc. The resulting spectrum is shown by the grey line in Fig. 1. Note that the cascade is sufficiently developed for $E_p \gtrsim 40$ EeV, the GZK energy. Hence, the spectrum depends more on the propagation effects than on the source parameters. The upcoming γ -ray detector Cherenkov Telescope Array (CTA) will detect γ rays in the range from 20 GeV up to several hundred TeV, with unprecedented sensitivity. The orange dashed curve in Fig. 1 shows the differential point source sensitivity of CTA, assuming 50h observation time and pointing to 20 degrees zenith (Gueta 2021). CTA observation of a hard and non-variable multi-TeV γ -ray spectrum will indicate the presence of UHECR acceleration inside this source. The blue dashed line is the LHAASO 1-yr sensitivity to Crab-like γ -ray point sources (Vernetto 2016).

We define the line-of-sight resolved component of the cosmogenic γ -ray spectrum as the fraction of UHECRs (ξ_B) that survives within 1° of the initial propagation direction, from the source to the observer, after deflection in the EGMF. For neutrinos of energy ~ 30 TeV, the angular resolution of IceCube

for track-like events is $\sim 0.5^\circ$. Whereas, Fermi-LAT has a resolution of 3.5° to photons of energy < 100 MeV, and $\sim 0.15^\circ$ beyond 10 GeV. We use CRPropa-3 to propagate UHECRs in the extragalactic space (Alves Batista et al. 2016). ξ_B is calculated from the arrival direction of protons in a 3D simulation on the surface of a sphere of radius 100 kpc, centered at the observer. We propagate a E^{-2} proton spectrum in the energy range between 0.1 and 100 EeV in a random turbulent magnetic field with a Kolmogorov power spectrum. The coherence length of the field is adjusted to 100 kpc. Thus, the secondary flux for a given luminosity is multiplied by ξ_B to obtain the line-of-sight component at the position of the observer (Das et al. 2020). The survival fraction ξ_B as a function of rms field strength is shown in Fig. 2.

The value of B_{rms} can be constrained from the required luminosity in cosmogenic γ -rays by the following expression, under isotropic approximation

$$\frac{L_{\text{UHEP}}}{4\pi d_L^2} = \frac{1}{\xi_B f_{\gamma,p}} \int_{\epsilon_{\gamma,\min}}^{\epsilon_{\gamma,\max}} \epsilon_\gamma \frac{dn}{d\epsilon_\gamma dAdt} d\epsilon_\gamma \quad (9)$$

where $dn/d\epsilon_\gamma dAdt$ is the differential flux of cosmogenic γ rays constrained by the SED. We calculate the electromagnetic cascade using the external code DINT integrated with CRPropa-3 (Heiter et al. 2018). The factor $f_{\gamma,p}$ takes into account the fraction of injected UHECR power that goes into cosmogenic γ rays and is fairly constant with the variation of B_{rms} . For TXS 0506+056 we find $f_{\gamma,p} \approx 0.156$. The integrated flux of cosmogenic photons along the line-of-sight of the observer, allowed by the observed SED is $\sim 1 \times 10^{-11}$ erg cm $^{-2}$ s $^{-1}$, as found from Fig. 1. The luminosity of protons interacting inside the jet is found to be $L_p = 1.6 \times 10^{48}$ erg/s (cf. Tab. 1). Using the same normalization for the escaping proton spectrum beyond 0.1 EeV, the luminosity in UHECR protons, i.e., between 0.1 – 100 EeV is $L_{\text{UHEP}} \approx 8 \times 10^{47}$ erg/s. This implies from Eq. (9), for the allowed flux of cosmogenic γ rays, $\xi_B \lesssim 0.05$. This indicates an EGMF with RMS value higher than few times 10^{-5} nG as seen from Fig. 2. There may be no cosmogenic component along the line of sight for magnetic field strength much larger than this, otherwise, the luminosity budget is violated. It is to be noted, that this result is an order of magnitude estimate. The precise value is sensitive to the angular resolution to detect high energy γ -rays, the coherence length of EGMF, the angular spread of jet emission, and the numerical precision of cascade calculation.

We calculate the flux of cosmogenic neutrinos produced simultaneously during the propagation of UHECRs and use the same normalization as obtained for the allowed flux of cosmogenic γ -ray spectrum. The cosmogenic neutrino spectrum peaks at 2.8×10^{18} eV with peak flux $\sim 4.5 \times 10^{-13}$ erg cm $^{-2}$ s $^{-1}$, shown in Fig. 3. The IceCube-Gen2 detector will be capable of detecting neutrinos from TeV to EeV energies, with sensitivity five times larger than the currently operating IceCube experiment. We also show the 5σ sensitivity for detection of muon neutrino flux from TXS 0506+056, using the IceCube-Gen2 detector (Aartsen et al. 2021). The black and red lines correspond to 100 days and 10 years of observation and indicate the sensitivity for neutrino flares and the time-averaged neutrino emission, respectively. The neutrino flux is lower than the detection threshold, however. Thus the γ -rays provide more stringent limits on UHECR acceleration in TXS 0506+056.

4. Summary and Conclusions

The flux variability observed by MAGIC in December 2018 was very similar to that seen in 2017. No neutrino event was de-

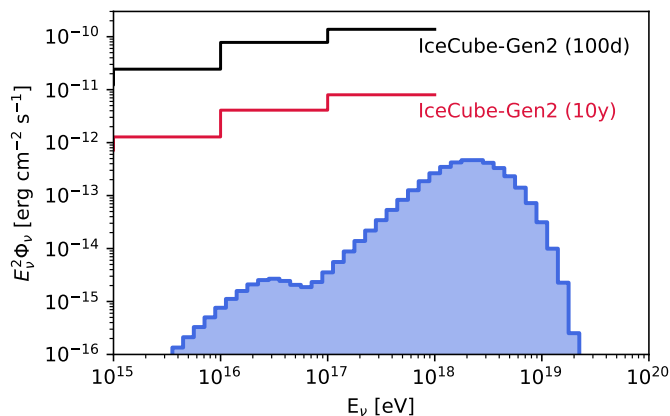


Fig. 3. All-flavor cosmogenic neutrino flux from TXS 0506+056 due to UHECR propagation along the line of sight, i.e., using the same normalization as the cosmogenic γ -ray spectrum in Fig. 1. The black and red curves correspond to 100 days and 10 years of observations of muon neutrino fluxes by IceCube-Gen2 and indicate the sensitivity for neutrino flares and the time-averaged neutrino emission, respectively.

tected in 2018 however, in contrast to the 2017 flare. In our one-zone modeling of the multiwavelength data from Nov 2017 - Feb 2019, we see that an increased γ -ray activity does not yield an increased neutrino flux, and the latter is comparable to the 7.5-yr flux prediction by IceCube, same as that obtained for the low state. Hence, the correlation between γ -ray and neutrino activity is subjective to the model undertaken. In our one-zone modeling we include three components, viz., the leptonic emission inside the jet, secondary emission due to hadronic cascade induced by protons ($E_p \lesssim 0.1$ EeV) and the line of sight resolved cosmogenic γ -rays due to propagation of UHECR protons ($E_p \gtrsim 0.1$ EeV) from the blazar to the Earth. The emission from the cascade is found to be sub-dominant in the GeV range but important in the X-ray and VHE bands. If the same physical process is responsible for the neutrino production, then the X-ray data constrains the neutrino flux to be consistent with IceCube prediction for one event in $\Delta T = 7.5$ yrs. Hence, an additional hidden sector must be invoked to explain a higher neutrino flux, for e.g., the neutrino flare in 2017 and $\Delta T = 0.5$ yr flux. This is consistent with no observation of γ -ray activity during the orphan neutrino flare during 2014-15.

We highlight our modeling as an important step in the course of study of TXS 0506+056, viz., (i) a neutrino flare (archival data) was observed in 2014-2015, but no gamma-ray activity, (ii) then an increased gamma-ray activity and simultaneous detection of a neutrino event in 2017 (iii) finally, no neutrino detection but increased gamma-ray activity in 2018. From the study of phase (iii), we show that indeed there is little correlation between gamma-ray and neutrino flares. Petropoulou et al. (2020) put an upper limit of $(0.4 - 2) \nu_\mu$ events in 10 years of IceCube operation, through multi-epoch modeling. They argue that the IC-170922A can be explained as an upward fluctuation from the average neutrino rate expected from the source, but in strong tension with the 2014–2015 neutrino flare. Rodrigues et al. (2019) shows only 2–5 neutrino events during the 2014-15 flare can be explained consistently with the X-ray constraints or high-energy γ -ray flux measured by Fermi-LAT. For all the cases presented in the two-zone model of Xue et al. (2019), the neutrino flux prediction is comparable to the 7.5-yr IceCube upper limit. In our study, the neutrino event rate is $N_{\nu_\mu + \bar{\nu}_\mu} = 1 \times (\Delta T / 7.5 \text{ yrs})$. Hence, along the lines of the one-zone leptohadronic model adopted

here, our results lead to similar conclusions using yet another epoch of the blazar and thus add to the literature.

The lack of simultaneous X-ray data in the high state is a drawback to the SED modeling, although the data points shown are that for the nearest observation on 2018 December 8. The parameters are varied minimally from the low state to account for this. Interestingly, our modeling does not predict any significant flare of the optical flux, where the SYN spectrum peaks, but the UV and soft X-ray fluxes are expected to change moderately. We note that a higher X-ray flux can allow for an increased neutrino flux, however. But explaining the $\Delta T = 0.5$ yr neutrino flux remains difficult due to excess X-ray production. Many plausible alternatives exist in the literature, such as neutrino production near the supermassive black hole of the AGN, in accretion disk or corona (Stecker 2013; Abbasi et al. 2022), or multiple emission zones with increased $\gamma\gamma$ opacity in the neutrino production zone (Xue et al. 2021), etc. Nevertheless, production of one neutrino event in 0.5-yr is achieved in Cerruti et al. (2019); Fraija et al. (2020), etc., but the neutrino flux peak is shifted compared to the mean energy of the observed event.

The origin of external photons is a question of fundamental importance in the modeling of TXS-like blazars. In their modeling, MAGIC collaboration used an external field originating from the spine layer or the jet-sheath (Ansoldi et al. 2018; Acciari et al. 2022). In our analysis, we consider it to originate from the BLR. It provides a substantial target for neutrino production by $p\gamma$ processes and also inverse-Compton scattering by electrons. For this to be true, the radius of the emission region must be smaller than the radius of the BLR region. In our analysis, R_{ext} is few times $\sim 10^{18}$ cm, which is large compared to usual estimates for the BLR region, $R_{\text{BLR}} = 10^{17} L_{\text{disk},45}^{0.5}$ cm (see Eqn. 4 in Ghisellini & Tavecchio 2008). One possibility is that the blob lies at the edge or even outside the BLR region leading to a decrease in the effective BLR photon density (Tavecchio & Ghisellini 2008). The typical energy of the photons in the AGN frame is $\epsilon_{\text{ext}} \sim 3k_B T' / \Gamma \approx 17$ eV. This is comparable to that obtained in other studies (Keivani et al. 2018) and can also be considered as scattered emission from the disk. The contribution from disk photon itself is negligible. We consider a log-parabola spectrum for the injection of electrons, to improve the fit to the observed SED. Often, other assumptions are also made in the literature, such as a broken power-law spectrum Xue et al. (2019).

In our modeling, for photohadronic interaction rate to dominate over escape, we need an escape timescale higher than $10^6(R/c)$ at ~ 1 PeV inside the emission region, and even higher at lower energies, assuming an energy-independent escape. In an energy-dependent parametrization, the escape timescale can be expressed as $t_{\text{esc}} \gg 10^6(R/c)(E/10^3 \text{ TeV})^{-1}$ for the proton energy range interacting inside the jet. In the one-zone model, the efficient escape of UHECRs require a rigidity-dependent diffusion rate, for e.g., $D(E) \propto E^2$ at higher energies (Globus et al. 2008; Harari et al. 2014; Muzio et al. 2022). As an alternative to the step function for the escape, as we had assumed, one may also assume a separate emission zone for acceleration of UHE protons with lower photohadronic opacity. We do not present the analytical estimates of such an astrophysical scenario in this paper, but assume a single proton population. In our analysis, the cosmogenic γ -ray spectrum remains fixed for both the low- and high-states. A change in the primary proton distribution will not affect the cosmogenic flux significantly, because the spectrum is driven greatly by parameters guiding the extragalactic propagation. Since UHECRs are delayed in the EGMF, any observed variability in the VHE regime occurs, most likely, due to an increased activity inside the jet. The required luminosity in

UHE protons can also be translated into a resulting flux of neutrinos at EeV energies. The cosmogenic neutrino flux predicted here, from constraints on γ -ray flux, is found to be lower than that in our earlier study (Das et al. 2022). Thus detection of cosmogenic neutrinos from TXS 0506+056 seems unlikely with the next generation upgrade of IceCube, leaving ground-based γ -ray detectors such as CTA to test UHECR signature in the SED of blazars.

Acknowledgements. S.D. thanks Konstancja Satalecka (MAGIC Collaboration) for correspondence regarding the multiwavelength SED data. The work of S.D. was supported by JSPS KAKENHI Grant Number 20H05852. Numerical computation in this work was carried out at the Yukawa Institute Computer Facility. S.R. was supported by a grant from NITheCS and the University of Johannesburg URC. We thank the anonymous referee for useful comments and suggestions.

References

- Aartsen, M. G. et al. 2018a, *Science*, 361, eaat1378
Aartsen, M. G. et al. 2018b, *Science*, 361, 147
Aartsen, M. G. et al. 2021, *J. Phys. G*, 48, 060501
Abbasi, R. et al. 2022, *Phys. Rev. D*, 106, 022005
Acciari, V. A. et al. 2022, *Astrophys. J.*, 927, 197
Alves Batista, R., Dundovic, A., Erdmann, M., et al. 2016, *JCAP*, 05, 038
Ansoldi, S. et al. 2018, *Astrophys. J. Lett.*, 863, L10
Banik, P. & Bhadra, A. 2019, *Phys. Rev. D*, 99, 103006
Boettcher, M., Reimer, A., Sweeney, K., & Prakash, A. 2013, *Astrophys. J.*, 768, 54
Cerruti, M., Zech, A., Boisson, C., et al. 2019, *Mon. Not. Roy. Astron. Soc.*, 483, L12, [Erratum: *Mon. Not. Roy. Astron. Soc.* 502, L21–L22 (2021)]
Chodorowski, M. J., Zdziarski, A. A., & Sikora, M. 1992, *ApJ*, 400, 181
Das, S., Gupta, N., & Razzaque, S. 2020, *Astrophys. J.*, 889, 149
Das, S., Gupta, N., & Razzaque, S. 2021, *Astrophys. J.*, 910, 100
Das, S., Razzaque, S., & Gupta, N. 2022, *Astron. Astrophys.*, 658, L6
Eichler, D. 1979, *Astrophys. J.*, 232, 106
Fraija, N., Aguilar-Ruiz, E., & Galván-Gómez, A. 2020, *Mon. Not. Roy. Astron. Soc.*, 497, 5318
Franckowiak, A. et al. 2020, *Astrophys. J.*, 893, 162
Gao, S., Fedynitch, A., Winter, W., & Pohl, M. 2019, *Nature Astron.*, 3, 88
Garrappa, S. et al. 2019, *Astrophys. J.*, 880, 880:103
Ghisellini, G. & Tavecchio, F. 2008, *Mon. Not. Roy. Astron. Soc.*, 387, 1669
Gilmore, R. C., Somerville, R. S., Primack, J. R., & Domínguez, A. 2012, *Monthly Notices of the Royal Astronomical Society*, 422, 3189
Globus, N., Allard, D., & Parizot, E. 2008, *Astron. Astrophys.*, 479, 97
Gould, R. J. & Schröder, G. P. 1967, *Phys. Rev.*, 155, 1404
Gueta, O. 2021, in *Proceedings of 37th International Cosmic Ray Conference — PoS(ICRC2021)*, Vol. 395, 885
Hahn, J. 2016, *PoS, ICRC2015*, 917
Harari, D., Mollerach, S., & Roulet, E. 2014, *Phys. Rev. D*, 89, 123001
Heiter, C., Kuempel, D., Walz, D., & Erdmann, M. 2018, *Astroparticle Physics*, 102, 39
IceCube Collaboration, Aartsen, M., et al. 2013, *Science*, 342, 1242856
Kalashev, O. E., Kusenko, A., & Essey, W. 2013, *Phys. Rev. Lett.*, 111, 041103
Keivani, A. et al. 2018, *Astrophys. J.*, 864, 84
Kelner, S. R. & Aharonian, F. A. 2008, *Phys. Rev. D*, 78, 034013, [Erratum: *Phys. Rev. D* 82, 099901 (2010)]
Kochocki, A., Takhistov, V., Kusenko, A., & Whitehorn, N. 2021, *Astrophys. J.*, 914, 91
Liu, R.-Y., Wang, K., Xue, R., et al. 2019, *Phys. Rev. D*, 99, 063008
Mücke, A., Engel, R., Rachen, J. P., Protheroe, R. J., & Stanev, T. 2000, *Computer Physics Communications*, 124, 290
Murase, K., Oikonomou, F., & Petropoulou, M. 2018, *Astrophys. J.*, 865, 124
Muzio, M. S., Farrar, G. R., & Unger, M. 2022, *Phys. Rev. D*, 105, 023022
Padovani, P., Oikonomou, F., Petropoulou, M., Giommi, P., & Resconi, E. 2019, *Mon. Not. Roy. Astron. Soc.*, 484, L104
Petropoulou, M., Dimitrakoudis, S., Padovani, P., Mastichiadis, A., & Resconi, E. 2015, *Mon. Not. Roy. Astron. Soc.*, 448, 2412
Petropoulou, M. et al. 2020, *Astrophys. J.*, 891, 115
Reimer, A., Boettcher, M., & Buson, S. 2019, *Astrophys. J.*, 881, 46, [Erratum: *Astrophys. J.* 899, 168 (2020)]
Rodrigues, X., Gao, S., Fedynitch, A., Palladino, A., & Winter, W. 2019, *Astrophys. J. Lett.*, 874, L29
Sahakyan, N. 2018, *Astrophys. J.*, 866, 109
Sahu, S., López Fortín, C. E., & Nagataki, S. 2020, *Astrophys. J.*, 898, 103
Sikora, M., Kirk, J. G., Begelman, M. C., & Schneider, P. 1987, *Astrophys. J. Lett.*, 320, L81
Stecker, F. W. 1968, *Phys. Rev. Lett.*, 21, 1016
Stecker, F. W. 2013, *Phys. Rev. D*, 88, 047301
Tavecchio, F. & Ghisellini, G. 2008, *Mon. Not. Roy. Astron. Soc.*, 386, 945
Vernetto, S. 2016, *J. Phys. Conf. Ser.*, 718, 052043
Xue, R., Liu, R.-Y., Petropoulou, M., et al. 2019 [arXiv:1908.10190]
Xue, R., Liu, R.-Y., Wang, Z.-R., Ding, N., & Wang, X.-Y. 2021, *Astrophys. J.*, 906, 51
Yuan, C., Murase, K., & Mészáros, P. 2020, *ApJ*, 890, 25
Zhang, B. T., Petropoulou, M., Murase, K., & Oikonomou, F. 2020, *Astrophys. J.*, 889, 118